Multimodal optical and Gd-based nanoparticles for imaging in inflammatory arthritis

J.S. Kim[1], H. An[2], W.J. Rieter[1], D. Esserman[3], K.M.L. Taylor-Pashow[1], R.B Sartor[4], W. Lin[2], W. Lin[1], T.K. Tarrant[5]

[1]Department of Chemistry, [2]Department of Radiology, [3]School of Medicine and School of Public Health, [4]Division of Gastroenterology and Hepatology, Department of Medicine, [5]Thurston Arthritis Research Center and the Department of Medicine, Division of Rheumatology, Allergy, and Immunology, University of North Carolina School of Medicine, Chapel Hill, USA.

Abstract

Objective

This report documents a multimodal nanoparticle (MNP) contrast agent, containing embedded luminophores and surface-immobilized gadolinium chelates, as a contrast agent of inflamed synovium in a collagen induced arthritis (CIA) model.

Methods

DBA-1J mice were immunized for CIA and imaged after disease onset by two independent modalities. After intravenous administration of MNP contrast, optical and magnetic resonance images were obtained and clinical disease was scored, which was followed by processing of hindlimbs for immunofluorescence and confocal microscopy.

Results

We show a correlation between disease severity and MNP optical luminescence that is dose dependent. Immunofluorescence of hindlimb sections reveal that MNP-labeled cells are monocytes/macrophages within the inflamed synovium. Magnetic resonance (MR) relaxation time maps, which determine the quantitative measure of T1 and T2 values at each imaging voxel, demonstrated a decreasing T2 signal in actively inflamed joints that was more pronounced earlier rather than later during disease.

Conclusions

MNPs containing surface-immobilized gadolinium chelates and embedded luminophores are potential dual-modality contrast agents in inflammatory arthritis and localize to monocytes/macrophages within inflamed synovium.

Key words

Nanostructures, arthritis, inflammation, magnetic resonance imaging, macrophages, monocytes, diagnostic imaging.

Jason S. Kim, PhD
Hongyu An, PhD
William J. Rieter, PhD
Denise Esserman, PhD
Kathryn M.L. Taylor-Pashow, PhD
R. Balfour Sartor, MD
Weili Lin, PhD
Wenbin Lin, PhD
Teresa K. Tarrant, MD

The experiments in this research were generously supported by the following funding mechanisms: the Thurston Arthritis Research Center at the University of North Carolina, the shared 9.4T MR instrumentation grant no. S10RR019924, and NIH grant no. P20 RR020764-01.

Please address correspondences and reprints requests to:
Teresa Tarrant, MD,
University of North Carolina at Chapel Hill, CB# 7280, 3300 Manning Drive, Chapel Hill, NC 27599, USA.
E-mail: tarra002@med.unc.edu

Received on September 5, 2008; accepted in revised form on March 16, 2009.

Competing interests: none declared.

Introduction

Magnetic resonance (MR) imaging has emerged as a powerful diagnostic tool owing to its non-invasive nature, intrinsically high spatial resolution, and reliance on non-radioactive contrast agents (1). In inflammatory arthridities such as rheumatoid arthritis, MR images give excellent soft tissue contrast that accurately depict derangements in synovium, cartilage, ligaments, menisci, and bony structures (2, 3). Although other imaging modalities have been explored in inflammation and arthritis, none have enhanced spatial resolution combined with structural information in the absence of radiation exposure as does MR (4). Given the powerful potential applications of MR, technologic advancement in the form of contrast-enhancing nanomaterials has been a rapid area of scientific investigation in the last decade. Previous studies using iron oxide nanomaterials in MR imaging have shown that these contrast agents are effective in inflammatory disease models including arthritis (5-7), insulinitis (8, 9), malignancy (10-12), atherosclerosis (13), and organ transplant and rejection (14). However, the development of diversified and multifunctional nanomaterials is still necessary for the continued advancement of this technology toward implementation in human disease.

In order to develop gadolinium-based contrast agents with enhanced sensitivity, Lanza *et al*. have developed a strategy of perfluorocarbon-based microemulsions coated with gadolinium (Gd)-chelates (15). In rheumatoid arthritis, Gd-based MR contrast agents are in widespread use due to their superior ability to distinguish synovial hypertrophy from inflammatory effusions (16) and their capacity to quantify inflamed synovium over time (17-19). Expanding from this microemulsion technology to a silica-based nanomaterial, we have developed a multimodal nanoparticle (MNP) contrast agent containing a $Ru(bpy)_3Cl_2$ core surrounded by a paramagnetic coating of Gd-DTTA silane derivative. This MNP contrast agent was shown previously by our group to have MR image capacity in addition to luminescent enhancement in mouse monocytes *in vitro* (20). Monocytes are critical to the disease pathogenesis of inflammatory arthritis (21) through antigen presentation and production of pro-inflammatory cytokines like TNF-α and IL-6, and have important pathophysiological roles in chronic disease states such as atherosclerosis (22) and malignancy (23). Based on our *in vitro* studies (20), the purpose of this study was to test our hypothesis that MNP contrast agents would label monocyte/macrophage cells within inflamed synovium in an *in vivo* inflammatory arthritis model, and that the labeling of these cells would predict disease activity.

Materials and methods

Animals

Animals used in these experiments were DBA-1J mice either purchased from Jackson Laboratories (Bar Harbor, ME) or bred and cared for in DLAM facilities under the approved IACUC protocol number 05-289.0 in pathogen free specific conditions.

Induction and evaluation of collagen-induced arthritis

Eight-week-old DBA-1J mice were immunized with adjuvant (Complete Freund's on day 0 and incomplete Freund's on day 21) ± 100μg per mouse of heterologous bovine type II collagen. Using a 27 gauge needle, 0.1 mL of a 1:1 mixture of adjuvant + collagen or saline was injected subcutaneously into the base of the tail. Specifically, 12 animals were immunized with Freund's adjuvant alone and did not develop arthritis; these served as controls to establish a baseline of autofluorescence emission for the paws in optical imaging studies. An additional 12 animals were immunized to develop CIA with the addition of 100 μg/mouse of type II bovine collagen emulsified in the Freund's adjuvant. All mice were scored by a rheumatologist, who was blinded to the contrast administration and image acquisition, for their severity of arthritis by two independent measures of clinical disease index and paw swelling. Clinical disease index was performed using the following scoring system: 0=normal paw; 1=mild but definite swelling of either the ankle or digits; 2=moderate redness and swelling of an ankle ± any number

of digits; 3=maximal redness and swelling of the entire paw and digits with or without ankylosis. The maximum score per paw was 3 with a total score obtainable of 12 per mouse. This scoring system has been validated by our (24) and other groups previously (25, 26). Paw swelling measurements were obtained by measuring the thickness of the fore- and hindlimbs at the wrist or ankle respectively. Paw swelling is presented as a change in the mean thickness of the mouse's fore- and hindlimbs (mm) from its baseline average.

Multimodal nanoparticle (MNP) contrast agent

The MNP contrast agent was prepared by the Lin group as previously described (20). Briefly, vigorously stirred luminophore-doped ($Ru(bpy)_3Cl_2$: excitation maxima 450 nm and emission maxima 595 nm) silicon dioxide nanoparticles prepared by water-in-oil reverse microemulsion were functionalized with Gd-(trimethoxysilylpropyl)diethylenetriamine tetraacetate. After purification, the hybrid contrast agent was dispersed in sterile saline (0.9%) solution for administration as a functional MNP contrast agent. In a clinical 3.0 Tesla MR imaging scanner, the $r1$ and $r2$ were measured to be 2.0 x 10^5 $(mM\ s)^{-1}$ and 6.1 x 10^5 $(mM\ s)^{-1}$ on a per MNP basis, respectively (20).

Immunofluorescence and histology

At experiment termination, hindlimbs were embedded in Tissue-Tek O.C.T and frozen in liquid nitrogen. 5-7 μm sections were cut from embedded hindlimbs using a CryoJane Cryostat, fixed, and then analyzed using a Zeiss LSM5 confocal laser scanning fluorescent microscope. Immunofluorescence of the cellular infiltrate located within the joint was performed with monoclonal antibodies targeting the following antigens; anti-B220 (B cell) (BD Biosciences, San Jose, CA) , -CD3 (T cell) (BD Biosciences, San Jose, CA) , -MOMA-2 (monocytes/macrophages) (donated as a kind gift from Beckman Coulter, Fullerton, CA).

Optical imaging of MNP contrast and data acquisition

In vivo fluorescence intensities of mouse paws were determined using a Xenogen IVIS 100 series Optical/Fluorescence Scanner with the excitation (445-490 nm) and emission (575-650 nm) filters. Twenty-four DBA-1J mice were immunized; 12 mice with type II bovine collagen (CIA) and 12 mice without (controls). Animals (n=4 per group) from the arthritis and control groups received by tail vein injection 0.05 mL of either saline, MNP low dose (125mg/kg), or MNP high dose (250mg/kg) in two doses separated by 6 hours on day 35 after immunization. Luminescence intensity of the paws was measured using an optical scanner with filters specific for the spectrum of the $Ru(bpy)_3Cl_2$ luminophore (excitation: 445-490 nm and emission: 575-650 nm) the following day. This particular luminophore was selected for our MNP contrast agent to distinguish between the autofluorescence that can occur from the collagen and elastin within the joint structures (27). Images were acquired 12 hours after the second injected dose of MNP contrast agent to ensure intravascular clearing of the contrast agent. Igor Pro 4.06 Living Image®, version 2.20.1 was used to record images, normalize background, and select regions of interest (ROIs) for luminescence quantification.

MR imaging and data analysis

MR imaging studies were acquired on a 9.4T Bruker BioSpec small animal scanner (Bruker Biospin, Ettlingen, Germany) with a 35 mm quadrature RF transmit and receive coil. Imaging of animals was performed under inhalational anesthesia with isofluorane (3% induction and 1% maintenance with a 5:1 mixture of air and O_2 at a constant flow rate of 600 ml/min). Two sets of images were obtained on 3 animals with CIA after the onset of clinical disease; one prior to MNP contrast injection and the second 12 hours after the last of 2 doses of contrast (125 mg/ml MNP) was administered intravenously via tail vein injection. A 3D Fast Low Angle Shot (FLASH) gradient echo sequence was utilized to obtain high resolution anatomical images of both legs and paws of an animal. The imaging parameters were as follows, TR/TE=120/2.876 ms, flip angle=30°, FOV=32*32*12 mm^3, Matrix Size=512*512*192, voxel size=0.062 x 0.062 x 0.062 mm^3. A 2D multiple echo spin echo sequence was used to estimate T2 maps. In total, 32 echoes with an echo spacing of 3.7 ms were obtained. The first echo time was 3.7 ms. TR was 2000ms. FOV and matrix size were set to 35x30 mm^2 and 128 x 128. The slice thickness was 1mm. T1 maps were obtained with a variable TR rapid acquisition relaxation enhanced (RARE) sequence with a TE=5.14ms. Twelve variable TRs (TR=50, 100, 300, 600, 1000, 1500, 2000, 2500, 3000, 4000, 5000, 7000 ms) were used with a FOV of 35x30 mm^2 and a matrix size of 128 x 128. RARE factor was 3. T1 and T2 maps were processed with the Image Sequence Analysis Tool of Bruker Paravision 4.0. In short, a curve was fitted to a equation $Y=A+C*(1-\exp(-TR/T1))$ to obtain T1 values. A single exponential decay curve fitting was performed to obtain T2 via $Y=A+C*\exp(-TE/T2)$.

Data analysis

The relationship between fluorescence and disease scores (clinical index or paw swelling) for each paw was analyzed using linear mixed models with fixed disease and random mouse effects. The methods of Lipsitz *et al.* (28) were used to calculate partial correlation coefficients adjusted for random mouse effects.

Results

In vivo optical images using MNP contrast agent correlate with the severity of inflammatory arthritis

We chose to investigate our MNP contrast agent in the Collagen Induced Arthritis mouse model (CIA) since this model shares several clinical, histopathological and immunological features with human rheumatoid arthritis, and is considered a robust model in which to investigate potential therapies (29). To investigate the optical contrast applications of our MNP nanoparticles in diseased and non-disease states, we imaged mice with and without CIA. Early after the onset of clinical arthritis (day 35), all controls (regardless of receiving MNP) and arthritic mice injected with normal saline (Fig. 1A-D) had minimal fluorescence compared

to those with active disease (Fig. 1E, F). The level of luminescence intensity (ROI) correlated with the clinical disease index (Fig. 2A) and with paw swelling (Fig. 2B) in animals that received MNP contrast agent, and the strength of this relationship was dose dependent (Fig. 2). Specifically, the partial correlation coefficients, adjusted for random mouse effects, between luminescence and clinical disease index for arthritic mice treated with either saline, 125 mg/kg, or 250 mg/kg MNP were 0.76 (p=0.068), 0.82 (p=0.013) and 0.89 (p=0.002), respectively (Fig. 2A). The partial correlation coefficients between luminescence and paw swelling in mice treated with saline, 125 mg/kg, or 250 mg/kg MNP were 0.79 (p=0.050), 0.90 (p=0.001), and 0.91 (p<0.001), respectively (Fig. 2B).

MNP contrast agent decreases T2 signal enhancement in vivo during active inflammation

To investigate *in vivo* MR imaging capacity of the MNP contrast agent, MR images of the hindlimbs were obtained on day 35, early after the onset of clinical arthritis. No differences were observed in arthritic paws between the before- and after-MNP contrast administration on high resolution anatomical images (Fig. 3B, D). It was our hypothesis that cellular expression of MNP contrast agent within the joint may require increased sensitivity for detection; therefore, we further investigated the use of MR-relaxation maps, which determine the quantitative measure of T1 and T2 values at each imaging voxel. The post-contrast MR relaxation maps showed a T2 reduction of signal enhancement when compared to the pre-contrast images, which ranged from a 33-55% reduction in T2 values from the control pre-contrast image (Fig. 3A). The mean and standard deviation of T2 before and after MNP contrast administration was 26.1±3.2 ms (range 21-36 ms) and 16.4±- 2.2 ms (range 11-23 ms), respectively. There was little to no change in T1 values after MNP contrast administration (0-3%) (Fig. 3A); the mean and standard deviation of T1 before and after MNP administration was 1590±110 ms (range 1220-1790 ms) and 1620±142

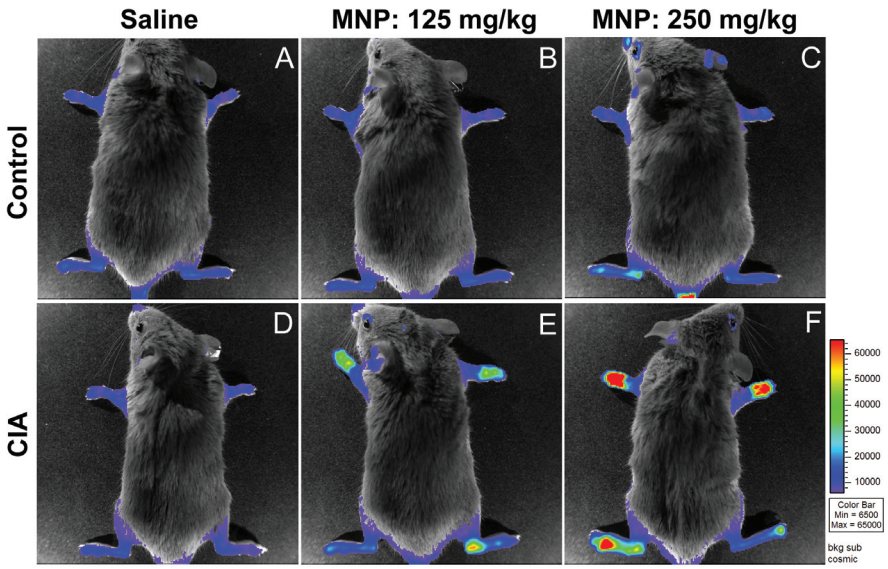

Fig. 1. Luminescence correlates with inflammatory arthritis after administration of multimodal nanoparticles (MNPs). The figure is a representative panel of an animal from each treatment group that was obtained using a Xenogen IVIS 100 series Optical/Fluorescence Scanner with the excitation (445-490 nm) and emission (445-490 nm) filters respectively. Control animals that did not have arthritis were intravenously injected with two separate doses of (**A**) saline, (**B**) 125 mg MNP/kg, or (**C**) 250 mg MNP/kg 12 hours before optical imaging. CIA immunized animals with arthritis were intravenously injected with (**D**) saline, (**E**) 125 mg MNP/kg, or (**F**) 250 mg MNP/kg in two separate doses on day 35 after the onset of arthritis and imaged 12 hours later.

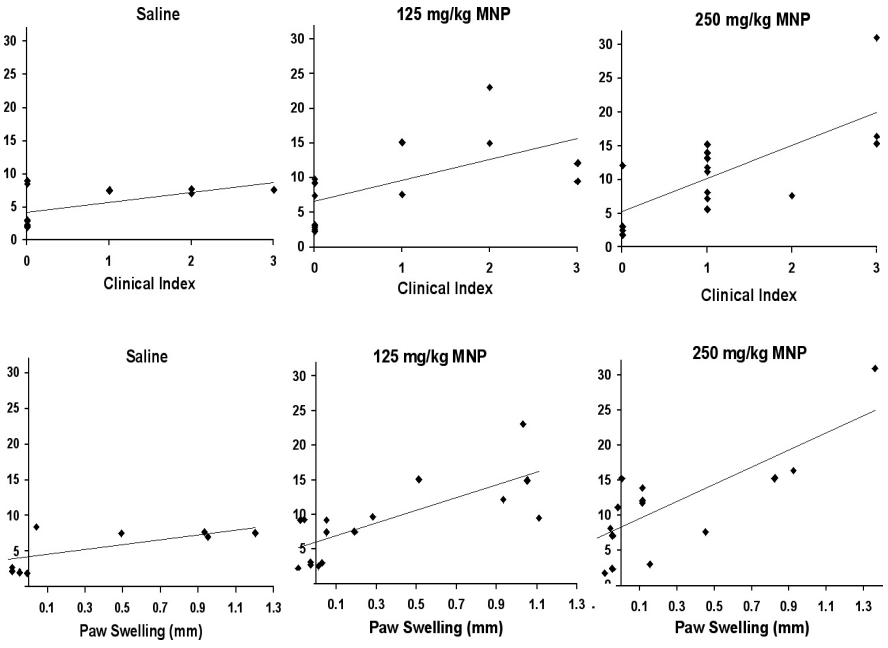

Fig. 2. *In vivo* optical images after MNP contrast agent administration correlate with the severity of inflammatory arthritis and are dose dependent. CIA immunized animals with arthritis were injected with saline, 125 mg MNP/kg, or 250 mg MNP/kg in two separate doses on day 35 after the onset of arthritis and imaged 12 hours later using a Xenogen IVIS 100 series Optical Scanner with the excitation (445-490 nm) and emission (575-650 nm) filters respectively. The level of luminescence intensity (ROI) *in vivo* correlated significantly to clinical disease index (**A**) and paw swelling (**B**) in animals that received MNP contrast agent, and the strength of this relationship was dose dependent. (**A**) The partial correlation coefficients, adjusted for random mouse effects, between luminescence and clinical disease index for arthritic mice treated with either saline, 125 mg/kg, or 250 mg/kg MNP were 0.76 (p=0.068), 0.82 (p=0.013) and 0.89 (p=0.002), respectively. (**B**) The partial correlation coefficients between luminescence and paw swelling in mice treated with saline, 125 mg/kg, or 250 mg/kg MNP were 0.79 (p=0.050), 0.90 (p=0.001), and 0.91 (p<0.001), respectively.

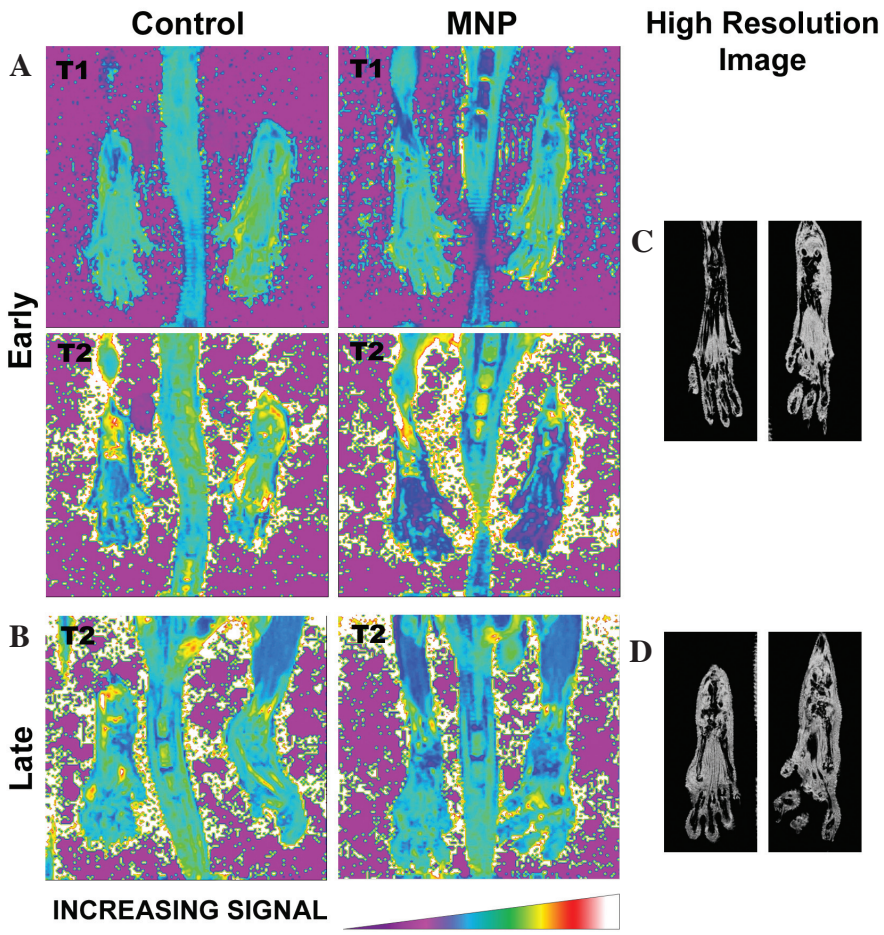

Fig. 3. MNP contrast agent decreases enhancement on T2, but not T1, relaxation maps in animals with inflammatory arthritis. (**A**) Representative T1 and T2 relaxation maps of the hindlimbs showing before (day 35) and after (day 36) MNP contrast agent in a mouse with early onset arthritis. The MNP contrast agent images were obtained 12 hours after injection with 2 separate doses of 125 mg MNP/kg. (**B**) T2 relaxation map of the hindlimbs from a mouse with later stage established disease before (day 50) and after (day 51) receiving MNP contrast agent. The MNP contrast agent images were obtained 12 hours after injection with 2 separate doses of 125 mg MNP/kg. T2-relaxation map signal enhancement is further reduced earlier (33-55% signal reduction) (**A**) rather than later (0-16% signal reduction) (**B**) in disease when compared to the control scan obtained prior to contrast administration.Panels (**C**) and (**D**) represent the corresponding high resolution MR images of early (day 35) and late (day 50) CIA.

ms (range 1150-2010 ms), respectively. We hypothesized from these images that the observed T2 changes might be reflective of MNP-labeled inflammatory cell infiltrates, and that this effect may be less pronounced at later disease stages when inflammation is resolving. To test this hypothesis, pre- and post-MNP contrast MR images were obtained in an animal with later staged-disease, approximately 2 weeks after the onset of clinical arthritis (day 50). Although T2 relaxation maps showed a reduction in signal enhancement in the arthritic paws (0-16%), it was substantially less pronounced (Fig. 3B) when compared to animals that were imaged early in the inflammatory process (Fig. 3A).

MNP contrast localizes to the inflamed synovial tissue and specifically labels macrophages

We had previously performed *in vitro* characterization and cellular viability studies on our MNP contrast agent (20). Consistent with our former findings that MNP contrast was non-toxic to hematopoetic cells, all mice that received MNP-contrast agent did not have adverse effects when observed up to 3 weeks after contrast administration.

Our previous *in vitro* characterization revealed that MNP contrast agent labeled macrophages with up to 99% efficiency (20), so it was our hypothesis that these cells would be preferentially labeled *in vivo*. To test this, we performed histopathology on tissue sections of the arthritic paws of animals that had received MNP contrast and evaluated them under fluorescent microscopy to localize the MNP. MNP contrast agent was found specifically in synovial tissue where active inflammatory disease had been present (Fig. 4) and was intracellular (Fig. 5). Immunofluorescent staining of hindlimb histopathology sections from CIA animals was performed to identify the following leukocyte antigens: MOMA-2 (monocyte/macrophage marker), B220 (B cell marker), and CD3 (T cell marker). When stained with either lymphocyte marker anti-CD3-FITC or anti-B220-FITC, joint sections showed no overlap with MNP contrast agent (Fig. 5). In contrast, the MNP luminescence was intracellular and within MOMA-2 positive leukocytes, consistent with monocyte/macrophage cells (Fig. 5).

Discussion

Current clinical studies have shown that T1 and T2 relaxation time mapping can identify pathophysiologic processes in joint disease (30-32). Our contrast agent detects both optical and T2 relaxation map differences in an arthritis model that correlates with disease activity. These studies suggest that a multimodal nanoparticle (MNP) contrast agent composed of a luminescent dye-doped silica nanoparticle with paramagnetic coating of Gd-DTTA silane derivative can be used as a sensitive noninvasive tool to monitor clinically relevant inflammation. Furthermore, the multifunctionality of the MNP luminescent core enabled us to demonstrate that monocytes/macrophages were preferentially labeled within the synovial tissue.

We had hypothesized that MNP contrast would label activated monocytes/macrophages either in the peripheral circulation leading to subsequent migration of these cells to the joints or via diffusion of MNP contrast into inflamed tissues via capillary leakage with subsequent uptake by resident synovial macrophages. It is likely that both mechanisms of target delivery occur *in vivo*, and as a result, activated synovial macrophages are labeled with high efficiency.

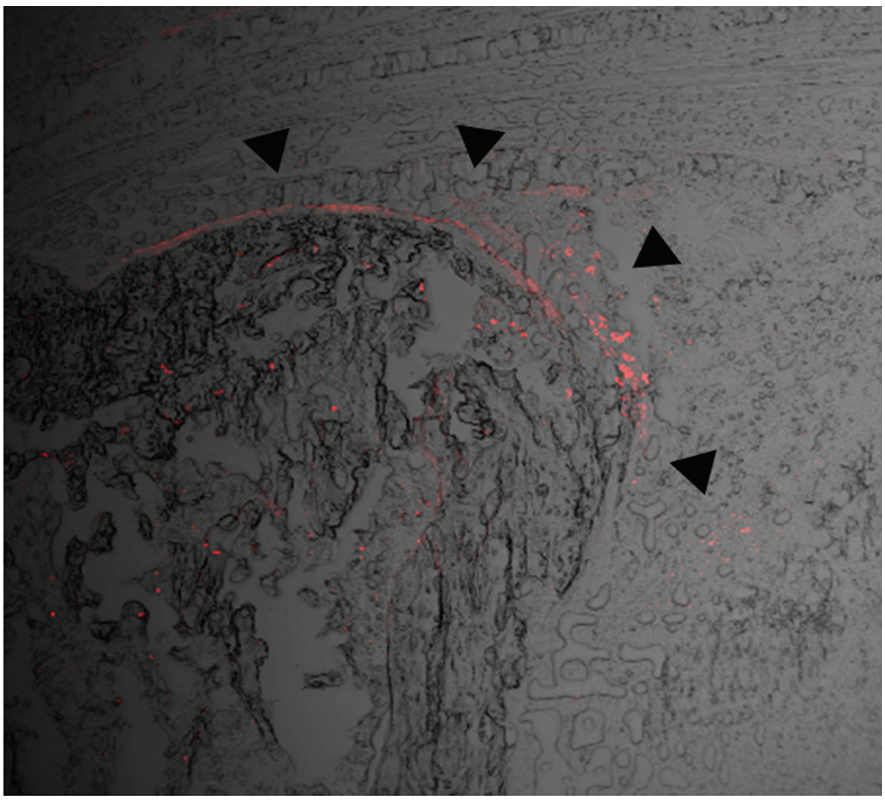

Fig. 4. Overlay of 10X light and fluorescence images from the hindlimbs of CIA animals showed MNP that localizes to the synovium (▲) of mice with inflammatory arthritis.

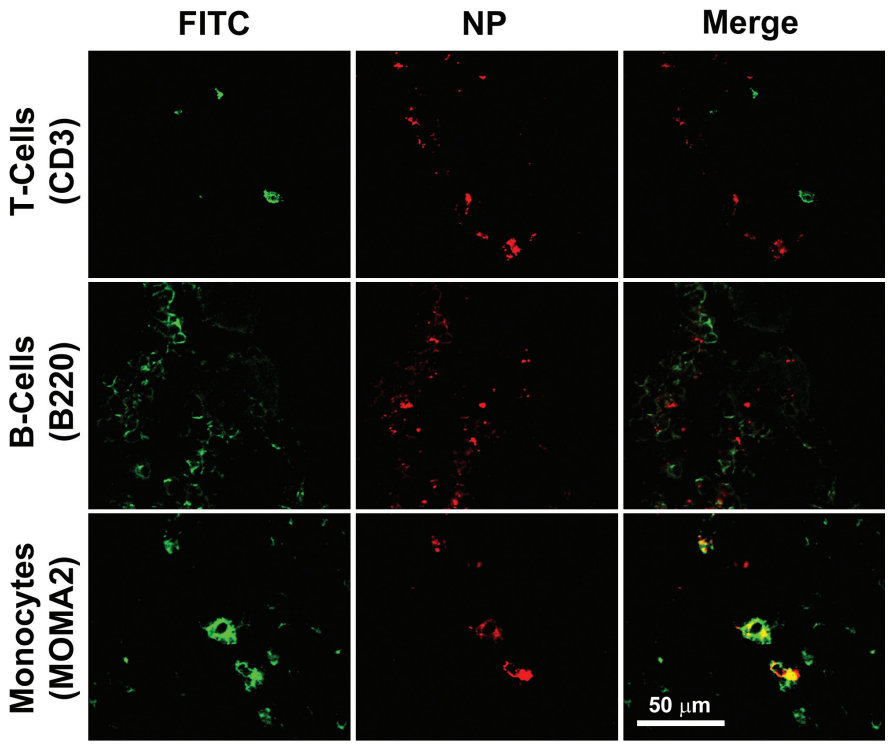

Fig. 5. Immunofluorescence of cyropreserved hindlimbs from arthritic mice demonstrates that MNP contrast is intracellular and specific for monocytes/macrophages. Tissue sections of the joints of CIA animals given MNP injections were examined under confocal microscopy at 63X magnification. MNP contrast agent was concentrated within the synovial tissue. Macrophages stained with a FITC conjugated anti-MOMA-2 marker had overlapping fluorescence with intracytoplasmic MNP, whereas lymphocytes (anti-CD3 and anti-B220 markers) did not.

Activated synovial macrophages have already been suggested as a potential biomarker in rheumatoid arthritis since their presence in human synovial tissue is highly correlated with radiographic disease progression (33) and their decreased presence in synovial tissue correlates with clinical remission (34). MNP contrast labeled arthritic paws correlated with the degree of disease activity, which suggests that this technology could be used to noninvasively monitor patients in response to treatment with a degree of sensitivity and specificity that does not currently exist in clinical practice.

Acknowledgements

The authors would like to thank the Michael Hooker Microscopy Facility, Dr Yonglong Hong for technical assistance with MR imaging, Nick Calderone and Dr David M. Lee for technical expertise of tissue slices, and Dr David Siderovski for his critical appraisal of the manuscript.

References

1. BUDINGER TF, LAUTERBUR PC: Nuclear magnetic resonance technology for medical studies. *Science* 1984; 226: 288-98.
2. MCQUEEN F, LASSERE M, EDMONDS J *et al.*: OMERACT Rheumatoid Arthritis Magnetic Resonance Imaging Studies. Summary of OMERACT 6 MR Imaging Module. *J Rheumatol* 2003; 30: 1387-92.
3. XIE X, WEBBER CE, ADACHI JD *et al.*: Quantitative, small bore, 1 Tesla, magnetic resonance imaging of the hands of patients with rheumatoid arthritis. *Clin Exp Rheumatol* 2008; 26: 860-5.
4. BABYN P, DORIA AS: Radiologic investigation of rheumatic diseases. *Pediatr Clin N Am* 2005; 52: 373-411, vi.
5. LUTZ AM, SEEMAYER C, COROT C *et al.*: Detection of synovial macrophages in an experimental rabbit model of antigen-induced arthritis: ultrasmall superparamagnetic iron oxide-enhanced MR imaging. *Radiology* 2004; 233: 149-57.
6. LUTZ AM, GOPFERT K, JOCHUM W *et al.*: USPIO-enhanced MR imaging for visualization of synovial hyperperfusion and detection of synovial macrophages: preliminary results in an experimental model of antigen-induced arthritis. *J Magn Reson Imaging* 2006; 24: 657-66.
7. DARDZINSKI BJ, SCHMITHORST VJ, HOLLAND SK *et al.*: MR imaging of murine arthritis using ultrasmall superparamagnetic iron oxide particles. *Magn Reson Imaging* 2001; 19: 1209-16.
8. TURVEY SE, SWART E, DENIS MC *et al.*: Noninvasive imaging of pancreatic inflammation and its reversal in type 1 diabetes.

J Clin Invest 2005; 115: 2454-61.

9. DENIS MC, MAHMOOD U, BENOIST C *et al.*: Imaging inflammation of the pancreatic islets in type 1 diabetes. *Proc Natl Acad Sci U S A* 2004; 101: 12634-9.
10. WEISSLEDER R, MOORE A, MAHMOOD U *et al.*: In vivo magnetic resonance imaging of transgene expression. *Nat Med* 2000; 6: 351-5.
11. MOORE A, MARECOS E, BOGDANOV A *et al.*: Tumoral distribution of long-circulating dextran-coated iron oxide nanoparticles in a rodent model. *Radiology* 2000; 214: 568-74.
12. HARISINGHANI MG, BARENTSZ J, HAHN PF *et al.*: Noninvasive detection of clinically occult lymph-node metastases in prostate cancer. *N Engl J Med* 2003; 348: 2491-9.
13. JAFFER FA, NAHRENDORF M, SOSNOVIK D *et al.*: Cellular imaging of inflammation in atherosclerosis using magnetofluorescent nanomaterials. *Mol Imaging* 2006; 5: 85-92.
14. WU YL, YE Q, FOLEY LM *et al.*: In situ labeling of immune cells with iron oxide particles: an approach to detect organ rejection by cellular MRI. *Proc Natl Acad Sci U S A* 2006; 103: 1852-7.
15. LANZA GM, WINTER PM, CARUTHERS SD *et al.*: Nanomedicine opportunities for cardiovascular disease with perfluorocarbon nanoparticles. *Nanomed* 2006; 1: 321-9.
16. VAN DER HEIJDE DM, VAN 'T HOF M, VAN RIEL PL *et al.*: Development of a disease activity score based on judgment in clinical practice by rheumatologists. *J Rheumatol* 1993; 20: 579-81.
17. CIMMINO MA, INNOCENTI S, LIVRONE F *et al.*: Dynamic gadolinium-enhanced magnetic resonance imaging of the wrist in patients with rheumatoid arthritis can discriminate active from inactive disease. *Arthritis Rheum* 2003; 48: 1207-13.
18. OSTERGAARD M, LORENZEN I, HENRIKSEN O: Dynamic gadolinium-enhanced MR imaging in active and inactive immunoinflammatory gonarthritis. *Acta Radiol* 1994; 35: 275-81.
19. OLIVER C, SPEAKE S, WATT I *et al.*: Advantages of an increased dose of MRI contrast agent for enhancing inflammatory synovium. *Clin Radiol* 1996; 51: 487-93.
20. RIETER WJ, KIM JS, TAYLOR KM *et al.*: Hybrid silica nanoparticles for multimodal imaging. *Angew Chem Int Ed* 2007; 46: 3680-2.
21. DE RYCKE L, BAETEN D, FOELL D *et al.*: Differential expression and response to anti-TNFalpha treatment of infiltrating versus resident tissue macrophage subsets in autoimmune arthritis. *J Pathol* 2005; 206: 17-27.
22. LIBBY P: Inflammation in atherosclerosis. *Nature* 2002; 420: 868-74.
23. SICA A, BRONTE V: Altered macrophage differentiation and immune dysfunction in tumor development. *J Clin Invest* 2007; 117: 1155-66.
24. TARRANT TK, RAMPERSAD RR, ESSERMAN D *et al.*: Granulocyte chemotaxis and disease expression are differentially regulated by GRK subtype in an acute inflammatory arthritis model (K/BxN). *Clin Immunol* 2008; 129: 115-22.
25. INGLIS JJ, NOTLEY CA, ESSEX D *et al.*: Collagen-induced arthritis as a model of hyperalgesia: functional and cellular analysis of the analgesic actions of tumor necrosis factor blockade. *Arthritis Rheum* 2007; 56: 4015-23.
26. SONG H, QIAO F, ATKINSON C *et al.*: A complement C3 inhibitor specifically targeted to sites of complement activation effectively ameliorates collagen-induced arthritis in DBA/1J mice. *J Immunol* 2007; 179: 7860-7.
27. ANDERSSSON-ENGELS S, WILSON BC: *In vivo* fluorescence in clinical oncology: fundamental and practical issues. *J Cell Pharmacol* 1992; 3: 48-61.
28. LIPSITZ S.R. LT, IBRAHIM S, LIPSHULTZ S: A partial correlation coefficient and coefficient of determination for multivariate normal repeated measures data. *The Statistician* 2001; 50: 87-95.
29. HEGEN M, KEITH JC JR, COLLINS M *et al.*: Utility of animal models for identification of potential therapeutics for rheumatoid arthritis. *Ann Rheum Dis* 2008; 67: 1505-15.
30. DARDZINSKI BJ, LAOR T, SCHMITHORST VJ *et al.*: Mapping T2 relaxation time in the pediatric knee: feasibility with a clinical 1.5-T MR imaging system. *Radiology* 2002; 225: 233-9.
31. VAN BREUSEGHEM I, BOSMANS HT, ELST LV *et al.*: T2 mapping of human femorotibial cartilage with turbo mixed MR imaging at 1.5 T: feasibility. *Radiology* 2004; 233: 609-14.
32. VAN BREUSEGHEM I, PALMIERI F, PEETERS RR *et al.*: Combined T1-T2 mapping of human femoro-tibial cartilage with turbo-mixed imaging at 1.5T. *J Magn Reson Imaging* 2005; 22: 368-72.
33. MULHERIN D, FITZGERALD O, BRESNIHAN B: Synovial tissue macrophage populations and articular damage in rheumatoid arthritis. *Arthritis Rheum* 1996; 39: 115-24.
34. SMITH MD, KRAAN MC, SLAVOTINEK J *et al.*: Treatment-induced remission in rheumatoid arthritis patients is characterized by a reduction in macrophage content of synovial biopsies. *Rheumatology* (Oxford) 2001; 40: 367-74.